Magnetic properties of drilled bulk high-temperature superconductors filled with a ferromagnetic powder

Gregory P. Lousberg[1,5], J.-F. Fagnard[1,2], X. Chaud[3], M. Ausloos[4], P. Vanderbemden[1], and B. Vanderheyden[1]

[1] SUPRATECS, Department of Electrical Engineering and Computer Science (B28), University of Liège, Belgium
[2] CISS Department, Royal Military Academy, Belgium
[3] CNRS/CRETA/LNCMI, Grenoble/Toulouse, France
[4] SUPRATECS (B5a), University of Liège, Belgium
[5] FRS-FNRS fellowship

E-mail: B.Vanderheyden@ulg.ac.be

Abstract.

It is shown that filling the holes of a drilled bulk high-temperature superconductor (HTS) with a soft ferromagnetic powder enhances its trapping properties. The magnetic properties of the trapped field magnet are characterized by Hall probe mapping and magnetization measurements. This analysis is completed by a numerical model based on a 3D finite-element method where the conductivity of the superconducting material is described by a power law while the permeability of the ferromagnetic material is fixed to a given value and is considered uniform. Numerical results support the experimental observations. In particular, they confirm the increase of trapped flux that is observed with Hall probe mapping after impregnation.

PACS numbers: 74.25.Ha,74.25.Sv

Submitted to: *Supercond. Sci. Technol.*

Keywords: trapped field magnet, drilled HTS, ferromagnetic/HTS hybrid structure, finite-element

1. Introduction

Recent progress in the synthesis of bulk high-temperature superconductors (HTS) with high current densities makes them very attractive to be used as permanent magnets in several engineering applications [1, 2]. Single domains of (RE)BCO, where RE denotes a rare earth, are able to trap up to 2 T at liquid nitrogen temperature [3, 4, 5], a trapped flux which is typically four times stronger than that measured above a Nd-based permanent magnet.

Trapped field magnets (TFM) are usually processed in either a parallelepiped or a disk geometry [6, 7, 8], have a typical length or diameter of 20 to 50 mm, and a thickness of 5 to 10 mm. In order to improve the processing of single domains with such large dimensions, it has been recently proposed to drill artificial holes in the sintered powder before the crystal growth [9, 10, 11]. These drilled structures offer a larger surface for oxygen diffusion, thus enabling a high oxygen content in the sample and reducing the formation of macrocracks during the oxygen annealing.

In drilled structures, the free space cleared by the holes may be advantageously used for TFM applications. As already discussed in Refs. [11, 12], the mechanical resistance of the magnet can be significantly increased by impregnating the holes with a resin. Similarly, the insertion of an iron yoke in the centre hole of an YBCO ring has been shown to increase the magnetic flux trapped by the ring [13]. These results suggest that the impregnation of the hole with a ferromagnetic material could be a simple way to enhance the trapped flux of the drilled sample.

Using a combination of ferromagnetic and HTS materials for enhancing the performance of an application is not a novel concept. Macroscopic hybrid ferromagnetic/superconducting structures have already been considered in various applications. When aimed at large current transport, HTS tapes that are surrounded by ferromagnetic sheets sustain larger critical currents with reduced AC losses [14, 15, 16, 17, 18, 19]. In magnetic shielding applications, placing a hollow ferromagnetic cylinder around a superconducting tube improves the shielding properties of the superconductor [20, 21, 22].

To our knowledge, the situation where the holes of a drilled YBCO sample are filled with a ferromagnetic powder has never been considered. In this paper, we propose to characterize the magnetic properties of such impregnated structures using both experiments and modelling: the distribution of magnetic flux and the average magnetization of the impregnated TFM are measured and compared to numerical results obtained with a three-dimensional finite-element method.

The paper is organized as follows. In Section 2, we present the techniques used for impregnating the samples and for measuring their magnetic properties. The experimental results are then discussed in Section 3. Section 4 reports on the numerical model for calculating the magnetic properties of impregnated samples. In Section 5, we describe the simulation results and use them for explaining the measurements. Section 6 summarizes our findings and presents our conclusions.

2. Experiment

2.1. Drilled samples and impregnation technique

We consider two drilled samples made out of bulk $YBa_2Cu_3O_{7-\delta}$ high-temperature superconductors (HTS). The samples were processed at CRETA (Grenoble, France) by the top-seeded melt-grown technique [10] in the shape of cylinders with a diameter of 16 mm and a height of 10 mm. Artificial holes were drilled in the preforms, in the direction parallel to the c-axis of the samples. Samples A and B were prepared with 55 holes each, with diameters of respectively 0.8 mm (sample A) and 0.35 mm (sample B). The holes were arranged on a centered rectangular lattice.

The magnetic properties were measured for each sample with and without a ferromagnetic material in the holes. Ideally, such a material should exhibit a high initial relative permeability, μ_r, and a high saturation density, B_s, both at cryogenic temperatures. The material should be easily manipulated in order to fill the holes compactly, the best option being a powder. In practice, one finds materials such as iron-nickel alloys with high μ_r ($\sim 10^4$) but small B_s ($< 500 - 800$ mT), or materials with larger B_s (> 1 T) but smaller μ_r.

As will be shown below, the trapped field magnets considered in this paper can trap magnetic fields with local densities of the order of 500 mT. We thus opted for a magnetic alloy [23], the stainless steel AISI 410 ($Fe/Cr_{12.5}$), which is available in the form of a powder, has a large saturation density of $B_s \sim 1.1$ T, and exhibits an initial permeability $\mu_r \sim 30$. The average size of the particles is 45 μm, which is much less

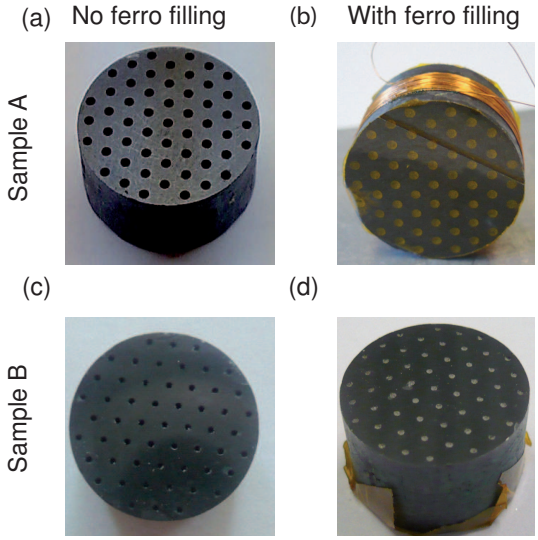

Figure 1. (a)- Picture of sample A before impregnation. (b)- Picture of sample A after impregnation. (c)- Picture of sample B before impregnation. (d)- Picture of sample B after impregnation.

than the diameter of the holes. The powder is compacted mechanically and held in the holes by two polyimide films (Kapton) placed on the sample surfaces.

The volume ratio of ferromagnetic powder in samples A and B is 16% and 3%, respectively. The relative magnetic permeability of the powder at low fields was measured as $\mu_r = 24$ at $T = 300$ K and as $\mu_r = 28$ at $T = 77$ K. Figure 1 shows a photograph of samples A and B before and after filling the holes with the ferromagnetic powder.

2.2. Experimental methods

To characterize the influence of the ferromagnetic powder on the magnetic properties of the drilled superconductors, two types of quantities were measured : (i), the average magnetization, and (ii), the distribution of the trapped magnetic flux above the surface of the sample.

2.2.1. Measurement of the average magnetization

The average magnetization of the drilled samples is measured in a Physical Property Measurement System (PPMS - Quantum Design). Fourty turns of 80 μm-diameter wire are wound around the sample. This constitutes a pick-up coil which is centered around the median plane and extends up to 3 mm from the bottom and top surfaces. The sample is inserted in the experimental chamber of the PPMS and is cooled down to 77 K in zero field. Then, a linearly increasing magnetic flux density, B_a, is applied parallel to the c-axis. The field is swept from 0 T to 1.5 T at a rate of 5 mT/s, and then cycled between -1.5 T and 1.5 T with the same sweep rate. The induced electromotive force (emf) across the pick-up coil is recorded by a nanovoltmeter (HP 34420A) controlled by a GPIB interface. The coil signal is calibrated by running a measurement sequence at a temperature of 100 K, when the sample is in the normal state.

The induced emf is integrated numerically in order to obtain the average flux density inside the sample, $< B >$. The magnetization M of the sample is then given by

$$\mu_0 M =< B > -B_a. \tag{1}$$

During the integration procedure, the constant offset of the voltmeter is carefully subtracted from the measured data, so that each magnetization curve is superposed on itself after a complete cycle.

2.2.2. Characterization of the trapped magnetic flux

The spatial distribution of the magnetic field above the sample is measured with a miniature probe, fixed to a motor-driven xy micro-positioning stage scanning over the sample surface. The active area of the Hall probe is 0.05×0.05 mm^2 and is sensitive to the component of the local field which is perpendicular to the surface. The gap between the Hall probe and the sample surface is maintained at 0.5 mm. The Hall probe is moved across either the top or bottom surface with a step size of 0.5 mm in the x and y directions. In addition to the distribution of the magnetic flux density above the surface,

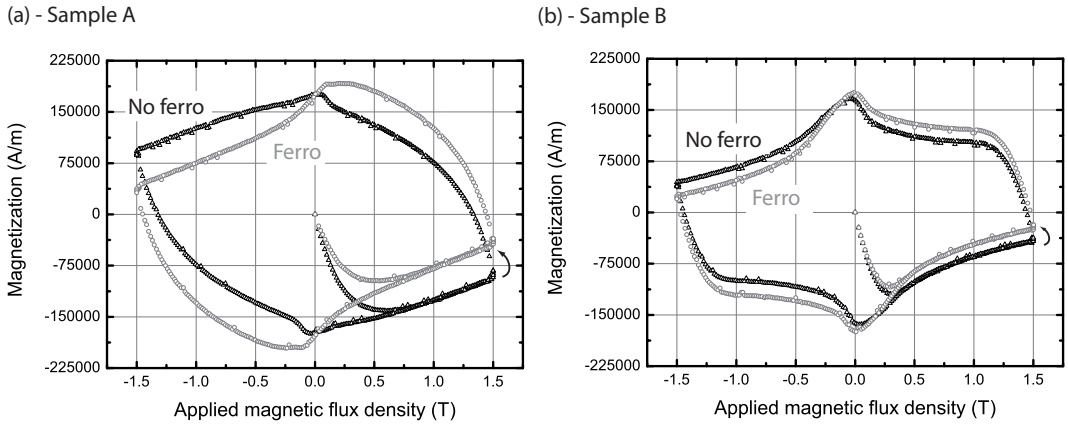

Figure 2. Volume magnetization as a function of the applied flux density of the non-impregnated (open black triangles) and the impregnated (open grey circles) samples.

we also measure the maximum trapped magnetic flux density directly on the surface. To this aim, we bring the Hall probe in close contact with the sample and the probe position is adjusted around the sample centre until the maximum value is recorded. The trapped field in the drilled samples is measured for 15 min, after a 5 min field-cooling activation in a uniform magnetic flux density of 500 mT generated by a large copper coil.

3. Experimental results

The average magnetization curves of samples A and B are shown in Figure 2-(a,b), respectively with (open grey circles) and without (open black triangles) the ferromagnetic powder in the holes. Each magnetization curve forms a hysteresis loop. In sample A, the impregnation of the holes strongly modifies the hysteresis loop, which undergoes a counter-clockwise rotation of a few degrees with respect to its centre (see arrow in Figure 2). The magnetization of sample A under large fields is strongly modified after impregnation. In particular, when $B_a = 1.5$ T, the bulk magnetization of the non-impregnated sample increases from $-100\ 000$ A/m to $-50\ 000$ A/m when the holes are filled with the powder. Note that the ferromagnetic filling also affects the shape of the magnetization curve, which develops an increase of the magnetization (in absolute value) on the upper right and lower left parts of the cycle. These changes are similar to those found for the iron-YBCO structure studied by Granados *et al* [13]. In sample B, the magnetization curve is modified in similar ways upon impregnation, although the magnitude of the counter-clockwise rotation is smaller than in sample A, consistent with a smaller volume proportion of the ferromagnetic material in sample B (3%) than in sample A (16%). In both samples, the average remnant magnetization is almost unaffected by the impregnation.

The distribution of the vertical component of the trapped magnetic flux density above the top and bottom surfaces of samples A and B is shown in Figure 3-(a,b). For

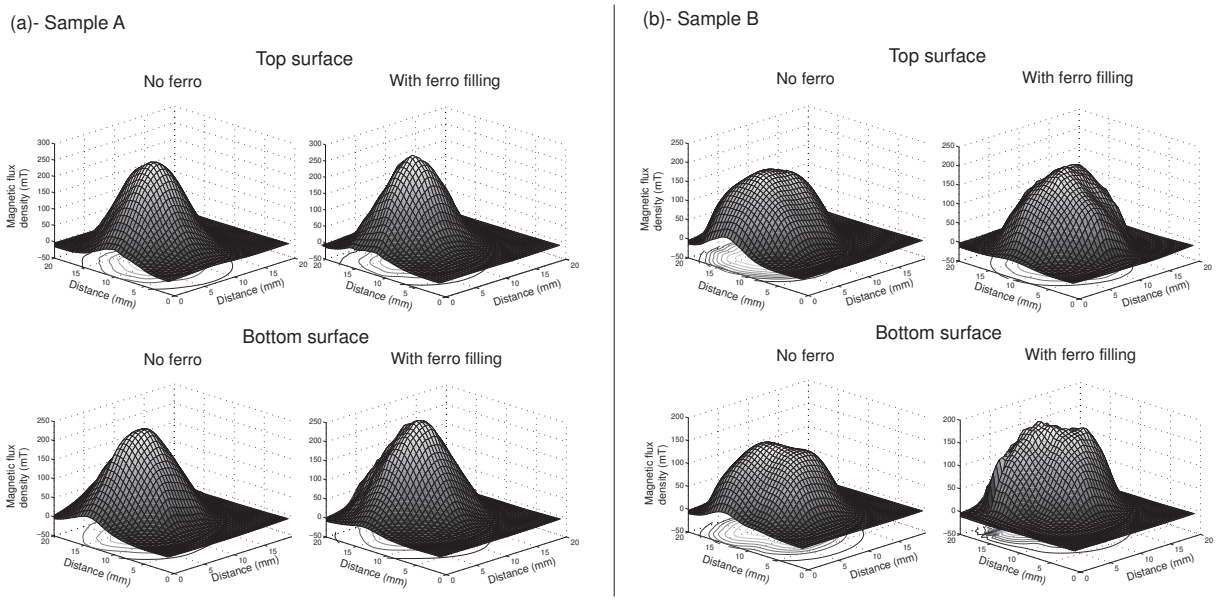

Figure 3. Hall probe mappings of the trapped flux density after a field-cooled magnetization (B_a = 450 mT) at 0.5 mm above the surface of the non-impregnated (left column) and impregnated (right column) samples. In each case, the first row corresponds to the top surface and the second one to the bottom surface.

each sample, the trapped flux distributions are shown either without (left panels) or with (right panels) ferromagnetic powder in the holes. As usual with this field mapping technique, the small but finite distance between the probe and the surface does not allow one to resolve the positions of the holes [24, 25].

As observed in Figure 3, filling the holes with the ferromagnetic powder leads to slight modifications of the trapped flux profiles. When there is no ferromagnetic material inside the holes, samples A and B exhibit an axisymmetric flux profile with a single maximum for both surfaces, indicating that there is no macrocrack close to the surfaces. In sample A, when the holes are filled with the powder, the maximum trapped flux that is measured at 0.5 mm above the surface is slightly larger than when the sample is not impregnated, while the flux profile is almost unchanged. In sample B, the impregnation of the holes involves a similar slight increase of the maximum trapped flux, and the corresponding flux distribution is irregular, with some bumps around the maximum. It should be noted that sample A appears to be of a better quality than sample B, as indicated by a larger trapped flux, already in the sample with no ferromagnetic filling.

In order to further investigate the increase of trapped flux observed in Figure 3, we report in Table 1 the maximum vertical component of the trapped flux density, $B_{\max}$, measured when the Hall probe is brought in contact with the surface. The impregnation of the holes in sample A yields the largest increase of trapped flux, with a relative increase of $\sim$ 34 % measured on the top surface. By contrast, the maximum trapped flux density of sample B rises by $\sim$ 10 %.

Table 1. Maximum trapped magnetic flux density on the top and bottom surfaces of Sample A and B

	Sample A		**Sample B**	
	No ferro	Ferro	No ferro	Ferro
Top surface	303 mT	406 mT	209 mT	244 mT
Bottom surface	282 mT	350 mT	176 mT	194 mT

4. Numerical model

Modelling the detailed behaviour of the hybrid system is a challenging task. As will be explained below, a number of simplifications are needed in order to keep a manageable number of unknowns and a reasonable resolution time. The following model is thus a qualitative one, which reproduces the systematic behaviour of the system and helps us elucidate the influence of the main parameters.

We follow the 3D finite-element method described in Ref. [27]. The magneto-quasistatic Maxwell equations are expressed in the $\mathbf{A} - \Phi$ formulation and solved with the *open source* solver GetDP. The HTS is modelled with a power law relationship between the electric field E and the current density J, $E = E_c(J/J_c)^n$, where E_c and J_c are respectively the critical electric field and the critical current density. Here, as a first approximation, J_c is taken constant.

The ferromagnetic material inside the holes is described with a specific magnetic constitutive law that should ideally include both saturation and the variation of μ_r with B. (The magnetic permeability is defined piecewise on the simulation domain and is discontinuous at the superconductor/powder interface.) However, incorporating a non-linear ferromagnetic constitutive law in the 3D finite-element formulation leads to time-consuming calculations. As an example, a non-linear magnetic permeability has already been successfully integrated in GetDP when modelling F/S hybrid structures for the specific case of two-dimensional axisymmetric geometries that we discussed in our previous work [22]. In such geometries, the meshing comprises less than 5000 nodes and the treatment of the non-linearity of the magnetic material requires a calculation time that is 20 times larger than that required if the material is linear. Such an increase in the time cost is not affordable in the 3D meshings of the present work, involving over 150000 nodes.

The results obtained in Ref. [22] concerning the shielding properties of a combination of a superconducting tube with a ferromagnetic one show that the saturation of the ferromagnetic material does not *qualitatively* modify the results. An enhancement of the shielding limit of the superconducting tube is still observed, even though the saturation alters the actual value of the relative increase of the shielding limit.

In our problem, we expect that modelling the ferromagnetic powder with a field-

independent magnetic permeability should already bring very valuable qualitative results. As the saturation of the ferromagnetic material is accompanied by a decrease of its relative magnetic permeability μ_r (approaching asymptotically $\mu_r = 1$ at large magnetic fields) a simple way to estimate the effects of the saturation is to consider a constant magnetic permeability that is smaller than the low field value. To this aim, three different values of magnetic permeability are considered (in a given simulation, a unique value of μ_r is assigned to the ferromagnetic region): (i) $\mu_r = 20$, which is close to the measured permeability of the ferromagnetic powder at low fields, (ii) $\mu_r = 2$, and (iii) $\mu_r = 1.5$. The last two values are representative of situations when the powder is saturated.

It should be noted that the magnetic flux density, and hence, the magnetic permeability of the ferromagnetic powder, is in fact a function of the radial position of the hole with respect to the sample centre and may also vary along the axis direction. Our use of a uniform magnetic permeability neglects these variations.

A further approximation consists in neglecting the electrical conductivity of the ferromagnetic material, σ. The characteristic time for the magnetic flux to diffuse across a hole with a diameter d is given by $\delta T = \pi\sigma\mu d^2$. This time is much shorter than the time taken by the external source to magnetize the system, $T = B_{\max}/\dot{B}_a$. For instance, taking $d = 0.8$ mm for sample A, $\sigma = 2.5\ 10^6$ S/m [26], $\mu = 30\ \mu_0$, and the values of Table 2, we find $\delta T = 0.2$ ms and $T = 300$ s. Retardation effects associated with eddy currents can thus be ignored and we set σ to zero.

As a final approximation, the magnetic behaviour of the ferromagnetic powder subjected to a given applied flux density, B_a, is assumed not to depend on the history of the applied field (we neglect the hysteresis of the soft ferromagnetic material). In particular, in the case of a linearly varying applied field, the simulation of the magnetic properties of the powder subjected to B_a should not depend on the number of time-steps. When associated with a HTS sample, single time-step simulations, as discussed in [27], are thus possible. In particular, two time-steps simulations are used for calculating the trapped flux profiles of impregnated samples, with a first step for increasing the applied flux density to $B_a = 3$ T at a sweep rate of 10 mT/s, and a second one for reducing the applied flux density to 0 with the same sweep rate.

The calculation is first performed on a geometry similar to that of sample A. The

Table 2. Parameters used for the finite-element simulations

Critical exponent	n	21
Critical current density	J_{c0}	$2\ 10^8$ A/m^2
Critical field	E_c	10^{-4} V/m
Maximum applied field	$B_{\max}$	3 T
Sweep rate	$\dot{B}_a$	10 mT/s

cylindrical sample has a height of 10 mm and a diameter of 16 mm. It contains 55 holes with a diameter that is either 0.8 mm (same as sample A), 1 mm, or 1.2 mm. In a second part, samples with different hole diameters are considered. The material parameters and the applied fields used in the simulations are summarized in Table 2.

5. Numerical results

5.1. Magnetization of impregnated samples

The virgin magnetization curve of the impregnated sample (diameter of the holes: 0.8 mm) is calculated with the help of FEM simulations. The applied field is ramped from 0 to $B_{\max}$ at a constant sweep rate, $\dot{B}_a = 10$ mT/s. Figure 4 shows the calculated magnetization M as a function of the applied field B_a for the non-impregnated sample ($\mu_r = 1$ - black line) and for the impregnated one with $\mu_r = 1.5$ (dark grey line), $\mu_r = 2$ (grey line), or $\mu_r = 20$ (light grey line). Each point of the magnetization curve is obtained with a single time-step FEM simulation. Note that the magnetization values corresponding to applied fields smaller than 600 mT suffer from bad convergence and are not reproduced in Figure 4.

The virgin magnetization curve of the non-impregnated sample saturates when $B_a > 800$ mT. In the impregnated samples, the magnetization no longer saturates at a constant value, but rather increases linearly with the applied field when $B_a > 800$ mT. The slope of the curve S, calculated between $B_a = 1$ T and $B_a = 3$ T, increases with the relative permeability of the powder: $S = 0.055$, $S = 0.066$, and $S = 0.62$, when $\mu_r = 1.5$, $\mu_r = 2$, and $\mu_r = 20$, respectively.

The magnetization curve of a drilled sample undergoes a counter-clockwise rotation

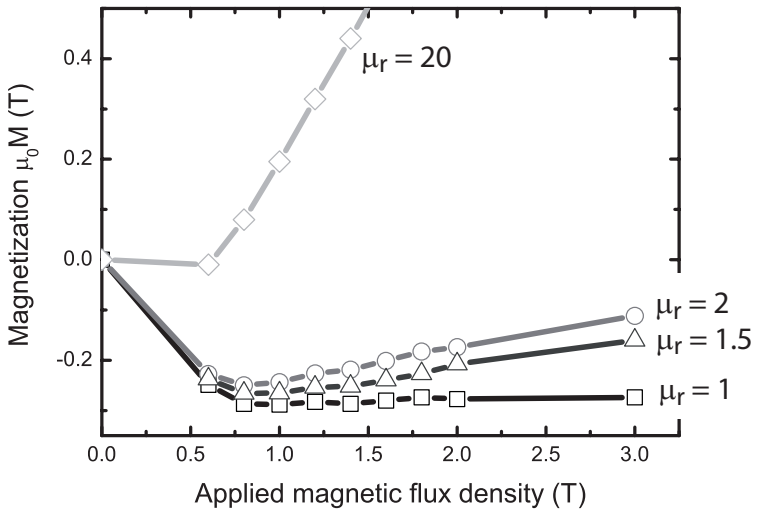

Figure 4. Initial magnetization curve of a drilled sample whose holes are either non-impregnated (black line) or impregnated with a ferromagnetic powder with μ_r =1.5 (dark grey line), μ_r =2 (grey line), and μ_r = 20 (soft grey line). The magnetization is calculated with a single time-step FEM simulation.

when the holes are filled with a ferromagnetic material. This tendency is consistent with the measured magnetization curve of the impregnated samples shown in Figure 2. Qualitatively, the increase of magnetization with the applied field that leads to the rotation of the magnetization curve results from the interplay between the diamagnetic behaviour of the superconductor and the ferromagnetic behaviour of the powder. The powder concentrates the flux lines inside the holes, thereby increasing the average flux density in the volume of the sample, as well as its average magnetization. The magnetic flux density inside the holes increases with the applied field, as indicated by the increase of the magnetization with the applied field.

Although the interplay between the superconducting and the ferromagnetic materials can be explained qualitatively in simple terms, we were unable to derive analytical expressions that quantitatively reproduce the numerical results. This difficulty arises from the fact that the magnetization of the impregnated holes directly affects — through demagnetizing effects — the magnetic flux threading the HTS bulk. Calculating the details of such an interaction requires numerical modelling.

5.2. Trapped flux profile in impregnated samples

The trapped flux profile along a diameter in the median plane of the drilled sample (diameter of the holes: 0.8 mm) is represented in Figure 5. The relative permeability of the ferromagnetic material is respectively $\mu_r = 1$ (non impregnated sample - black lines), $\mu_r = 2$ (dark grey lines), and $\mu_r = 20$ (grey lines). The hole positions are indicated by dashed lines. Note that, when $\mu_r = 20$, the magnetic flux density in several holes is in fact out of the range of the vertical axis.

At the interface between the superconductor and the ferromagnetic materials, the tangential component of the magnetic field $\mathbf{H}$ is continuous and the trapped flux profiles of impregnated samples exhibit discontinuities. In particular, the ratio between the magnetic flux density at the interface at the ferromagnetic side (with a relative permeability μ_r), B_{ferro}, and that at the superconducting side, B_{super}, is given as $B_{\text{ferro}}/B_{\text{super}} = \mu_r$. The magnetic flux density in the hole of the impregnated sample is thus larger than when the holes are not filled by the ferromagnetic powder. The increase of trapped magnetic flux density increases with the relative permeability of the ferromagnetic powder.

Moreover, the trapped magnetic flux profile in the superconductor is reshaped due to the presence of the ferromagnetic material inside the holes. The slope of the distribution of B between two neighbouring holes is reduced in the impregnated samples. In particular, the slope is smaller around the sample centre. This modification of slope in the trapped flux profile proves that the magnetization of the superconducting material is actually modified by the presence of the ferromagnetic powder in the holes.

From the results presented in Figure 5, we observe that the maximum trapped flux density is strongly enhanced in the median plane of the impregnated sample. However, such an increase is much larger than that observed on the surface with the Hall probe

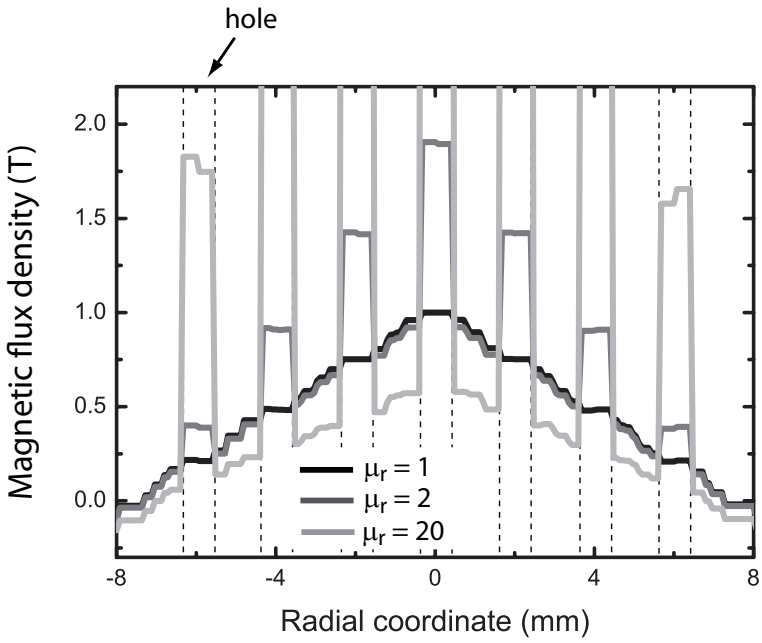

Figure 5. Trapped magnetic flux profile along a diameter in the median plane of a drilled sample, as calculated with two time-steps FEM simulations. The drilled sample is either non-impregnated (black line) or impregnated with a ferromagnetic powder of μ_r =1.5 (dark grey line) and μ_r =20 (grey line). The positions of the holes along the diameter are indicated by vertical dashed lines.

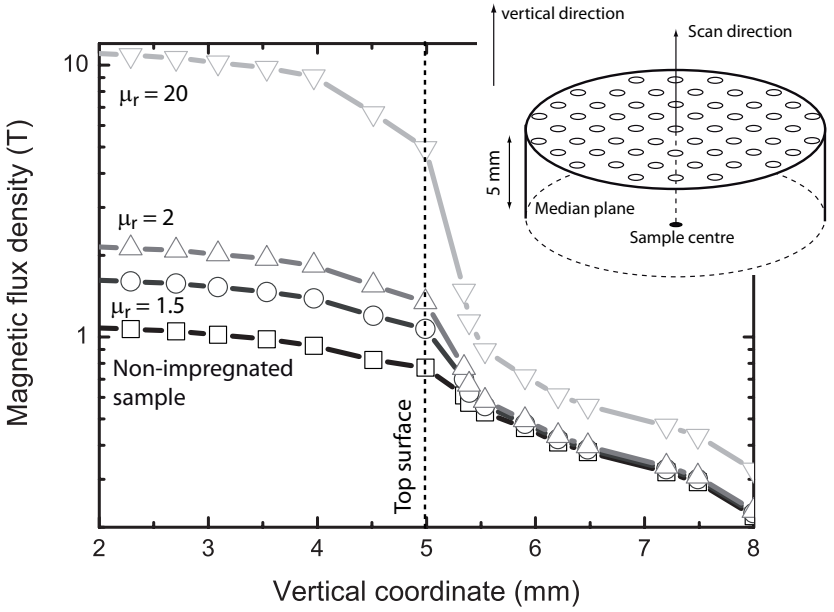

Figure 6. Vertical component of the trapped magnetic flux density as a function of the coordinate z, in a non-impregnated sample (black line) and in an impregnated sample with μ_r =1.5 (dark grey line), μ_r=2 (grey line), or μ_r =20 (light grey line).

mapping experiments reported in Figure 3.

Let us analyze the trapped flux density as one gets further from the median plane.

Table 3. Average trapped flux density in impregnated and non-impregnated samples

	Plain sample	**Drilled sample**	**Impregnated sample**		
			$\mu_r = 1.5$	$\mu_r = 2$	$\mu_r = 20$
Median plane	0.61 T	0.53 T	0.62 T	0.64 T	2.17 T
Top surface	0.5 T	0.41 T	0.49 T	0.53 T	1.9 T

In Figure 6, the vertical component of the magnetic flux density in the centre hole of the impregnated sample, B_z, is plotted as a function of the vertical distance from the median plane, z. The ferromagnetic material is assumed to be characterized by a constant relative permeability of $\mu_r = 1$ (non-impregnated sample - black line), $\mu_r = 1.5$ (dark grey line), $\mu_r = 2$ (grey line), or $\mu_r = 20$ (light grey line).

While the magnetic flux density remains almost constant in the volume of the ferromagnetic material (and equal to its value calculated in the median plane), it decays closer to the surface and drops suddenly above the sample surface ($z > 5$ mm) to get closer to the value of the non-impregnated sample. The magnitude of the drop increases with μ_r. As a result, the increase of trapped flux measured on the surface of the impregnated sample is lower than that calculated in the median plane. This contributes to the discrepancy between the increase of trapped flux density calculated in the median plane after impregnation and that measured experimentally above the surface.

The magnetic flux densities averaged over the cross section are calculated in the impregnated sample and in the non-impregnated one. They are listed in Table 3 for fields in the median plane and on the surface. While the average magnetic flux density in the median plane increases by a factor 1.17, 1.2, and 4 when the relative magnetic permeability is respectively $\mu_r = 1.5$, $\mu_r = 2$, and $\mu_r = 20$, the corresponding factors on the surface are given as 1.2, 1.3, and 4.63.

Table 3 also shows the average magnetic flux density calculated in a sample having the same characteristics as those of sample A but no hole. These values are of course higher in drilled samples [28]. In both the median plane and the top surface, we observe that the drop of the trapped flux density induced by the presence of the holes is totally compensated by impregnating the holes with the ferromagnetic powder, even with a relatively low magnetic permeability of $\mu_r = 1.5$. These results suggest that the impregnation of a drilled sample with a ferromagnetic powder allows one to reduce the inherent drop of trapped flux due to the presence of the holes, the magnitude of which was calculated in our previous works [27, 28].

Maximum local fields at 0.5 mm above the surface are listed in Table 4. A comparison of these increases of maximum trapped flux density with the measurements on sample A indicates that the ferromagnetic powder exhibits a relative permeability that is on average close to $\mu_r = 2$. This result indicates that most of the ferromagnetic powder is in fact saturated and, as a result, exhibits a small relative permeability.

Table 4. Maximum trapped flux density 500 μm above the top surface

Plain sample	**Drilled sample**	**Impregnated sample**		
		$\mu_r = 1.5$	$\mu_r = 2$	$\mu_r = 20$
0.72 T	0.56 T	0.6 T	0.64 T	1.07 T

Maximum trapped flux calculated at 500 μm above the top surface

Hole radius (mm)	0.4	0.5	0.6
Non-impregnated sample	560 mT	488 mT	420 mT
Impregnated sample (μ_r=2)	644 mT	574 mT	500 mT
Relative increase	15%	18%	19%

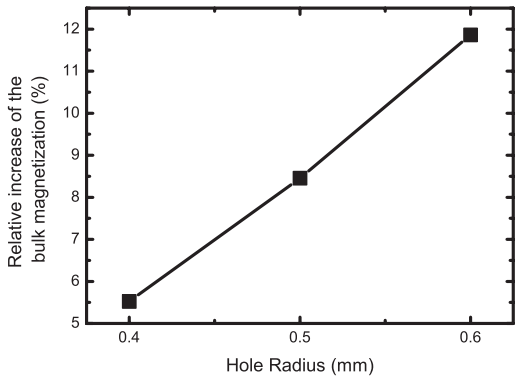

Figure 7. (a)- Maximum trapped magnetic flux density calculated 500 μm above the surface of a non-impregnated sample and an impregnated sample (μ_r =2). The hole radius is respectively 0.4 mm, 0.5 mm, and 0.6 mm. (b)- Relative increase of the trapped magnetization (with respect to that of a non-impregnated sample) as a function of the hole radius.

5.2.1. Influence of the volume of impregnated ferromagnetic material

Recall that the powder impregnation in sample B, with the smallest hole diameter, yields smaller modifications of the magnetic properties than those obtained with sample A (see Figure 3). In order to discuss this observation on the basis of our model, we consider three drilled samples with a different hole radius‡: (i) $r = 0.4$ mm – the same sample as that considered in the previous sections –, (ii) $r = 0.5$ mm, and (iii), $r = 0.6$ mm, where we assumed that a change in radius does not affect the J_c of the sample.

The maximum trapped flux density calculated 500 μm above the top surface is reported in Figure 7-(a). The samples are either impregnated (with a ferromagnetic material of relative permeability $\mu_r = 2$) or not. The relative increase with respect to a non-impregnated sample is also indicated. Figure 7-(b) shows the relative increase of the trapped magnetization in the impregnated samples (with respect to that of the non-impregnated ones) as a function of the hole radius. In each situation, we observe that the increase of trapped flux or magnetization depends on the volume of ferromagnetic powder inside the holes. The larger the hole radius, the larger the relative increase. Nevertheless, the increase of the hole radius is accompanied by a decay of the maximum

‡ Note that the modelling of a sample having a radius smaller than $r = 0.4$ mm (such as sample B) could not be performed because the size of the meshing exceeds the largest available computer capacity.

magnetic flux density that is trapped in the sample, since the volume of superconducting material is reduced.

Note that, in each case, the trapped magnetization of impregnated samples exhibits a smaller relative increase (as compared to a non-impregnated sample) than the maximum trapped flux. The effect of the ferromagnetic powder thus appears more pronounced when evaluating local quantities, such as the maximum trapped flux density, than when considering global quantities.

6. Conclusions

This paper presented the effects of filling the holes of drilled HTS samples with a ferromagnetic powder. These effects were both measured and evaluated with a FEM model.

The experimental and simulation results provided qualitative complementary observations that were in good agreement with one another (although the non-linearity of the ferromagnetic material is neglected in the model). They put forward two main consequences of impregnating the holes with a ferromagnetic powder:

(i) The magnetization curve of impregnated samples undergoes a counter-clockwise rotation with respect to that of a non-impregnated sample. The concentration of the flux lines inside the hole increases the average magnetic flux density in the sample and results in an increase of the average magnetization.

(ii) The trapped flux of impregnated samples is enhanced with respect to that of the non-impregnated ones. The increase of trapped flux is shown to be larger in the median plane than on the sample surface. The gain in the maximum trapped flux and in the magnetization of the impregnated samples could thus be used for reducing the inherent drop of trapped flux resulting from drilling holes.

The effects of the ferromagnetic material on the trapping properties of the drilled samples were found larger when the volume ratio of ferromagnetic material increases. Using holes of large diameters allows one to get a larger relative increase of the maximum trapped flux. However, there is a compromise to resolve as the samples with large hole diameters are not able to trap a large magnetic flux.

Our model was constructed with a number of simplifying assumptions. Two elements are worth discussing.

First, we showed that the enhancement of the trapping properties of drilled samples due to the ferromagnetic powder depends on its relative permeability. Our model thus predicts that a larger relative permeability leads to a larger relative increase of the trapped magnetization. It should however be kept in mind that the magnetization of the ferromagnetic material is bound to saturates for $B > B_s$, a flux density above which the powder exhibits a small effective permeability. Magnetic saturation of the ferromagnetic powder is expected to limit the predicted increases in magnetization.

Second, our model considered a constant current density J_c, whereas the sample clearly exhibited a $J_c(B)$ dependence. For samples with a strong variation of J_c with respect to B, the ferromagnetic material is expected to increase the trapped flux by two mechanisms: (i), by concentrating flux lines through the holes, as studied here, and (ii), by depleting the magnetic flux in the superconducting material, thereby increasing J_c and the magnetization.

In summary, our simplified model shows that a ferromagnetic material can be used to improve the trapped flux in a drilled bulk HTS.

7. Acknowledgments

This work has been partly funded by the *Fonds de la Recherche Scientifique (FRS-FNRS)* from Belgium and by the University of Liège.

References

[1] Campbell A M and Cardwell D A 1997 *Cryogenics* **37** 567

[2] Xu Y, Izumi M, Tsuzuki K, Zhang Y, Xu C, Murakami M, Sakai N and Hirabayashi I 2009 *Supercond. Sci. Technol.* **22** 095009

[3] Krabbes G, Fuchs G, Canders W, May H and Palka R 2006 *High Temperature Superconductor Bulk Materials*, Wiley-VCH, Berlin, p 109

[4] Fuchs G, Krabbes G, Mueller K-H, Verges P, Schultz L, Gonzalez-Arrabal R, Eisterer M and Weber H W 2003 *J. Low Temp. Phys.* **133** 159

[5] Weinstein R, Sawh R, Ren Y and Parks D 1998 *Mater. Sci. Eng. B* **53** 38

[6] Gawalek W, Habisreuther T, Zeisberger M, Litzkendorf D, Surzhenko O, Kracunovska S, Prikhna TA, Oswald B, Kovalev LK and Canders W 2004 *Supercond. Sci. Technol.* **17** 1185

[7] Nariki S, Sakai N, Kita M, Fujikura M, Murakami M and Hirabayashi I 2006 *Supercond. Sci. Technol.* **19** S500

[8] Cardwell D A and Hari Babu N 2006 *Physica C* **445-448** 1

[9] Noudem J G, Meslin S, Harnois C, Chateigner and Chaud X 2004 *Supercond. Sci. Technol.* **17** 931

[10] Chaud X, Isfort D, Porcar L, Tournier R 2005 *J. Eur. Ceram. Soc.* **25** 2955-2958

[11] Meslin S, Harnois C, Chubilleau C, Horvath D, Grossin D, Suddhakar E R and Noudem J G 2006 *Supercond. Sci. Technol.* **19** S585

[12] M. Tomita, M. Murakami 2003 *Nature* **421** 517

[13] Granados X, Torner M, Puig T and Obradors X 2007 *IEEE Trans. Appl. Supercond.* **17** 1629

[14] Gömöry F 2006 *Appl. Phys. Lett.* **89** 072506

[15] Mawatari Y 2008 *Phys. Rev. B* **77** 104505

[16] Majoros M, Glowacki B A and Campbell A M 2000 *Physica C* **334** 129

[17] Rupp S H, Caplin A D and Staines M P 2008 *J. Phys.: Conf. Ser.* **97** 012078

[18] Amemiya N and Nakahata M 2007 *Physica C* **463–465** 775

[19] Grilli F, Ashworth S P and Civale L 2007 *J. Appl. Phys.* **102** 073909

[20] Itoh M, Ohyama T, Hoshino K, Ishigaki H and Minemoto T 1993 *IEEE Trans. Appl. Supercond.* **3** 181

[21] Mori K, Minemoto T and Itoh M 1997 *IEEE Trans. Appl. Supercond.* **7** 378

[22] Lousberg G P, Fagnard J-F, Ausloos M, Vanderbemden P and Vanderheyden B 2010 *IEEE Trans. Appl. Supercond.* **20** 33

[23] Tavares S S M, da Silva M R, Neto J M, Miraglia S and Fruchart D 2002 *J. Magn. Magn Mater.* **242-245** 1391

[24] Lousberg G P, Fagnard J-F, Ausloos M, Vanderbemden P and Vanderheyden B 2010 *J. Phys.: Conf. Series* **234** 012023

[25] Meslin S, Harnois C, Chubilleau C, Horvath D, Grossin D, Suddhakar E R and Noudem J G 2006 *Supercond. Sci. Technol.* **19** S585

[26] A. F. Clark, G. E. Childs, and G. H. Wallace 1970, *Cryogenics* **10**, Issue 4, 295-305

[27] Lousberg G P, Ausloos M, Geuzaine C, Dular P, Vanderbemden P and Vanderheyden B 2009 *Supercond. Sci. Technol.* **22** 055005

[28] Lousberg G P, Ausloos M, Vanderbemden P and Vanderheyden B 2008 *Supercond. Sci. Technol.* **21** 025010